CONF-960401--5

LBL-38422
UC-401

Lawrence Berkeley Laboratory
UNIVERSITY OF CALIFORNIA

Accelerator & Fusion Research Division

To be presented at the Materials Research Society, San Francisco, CA, April 8–12, 1996, and to be published in the Proceedings

Angle-Resolved Photoemission Extended Fine Structure Study of Chemisorbed c(2×2)P/Fe(100): Comparison with Self-Consistent-Field Xα Scattered Wave Calculations

W.R.A. Huff, Y. Chen, X.S. Zhang, L.J. Terminello, F.M. Tao, Y.K. Pan, S.A. Kellar, E.J. Moler, Z. Hussain, H. Wu, Y. Zheng, X. Zhou, A.E. Schach von Wittenau, S. Kim, Z.Q. Huang, Z.Z. Yang, and D.A. Shirley

February 1996

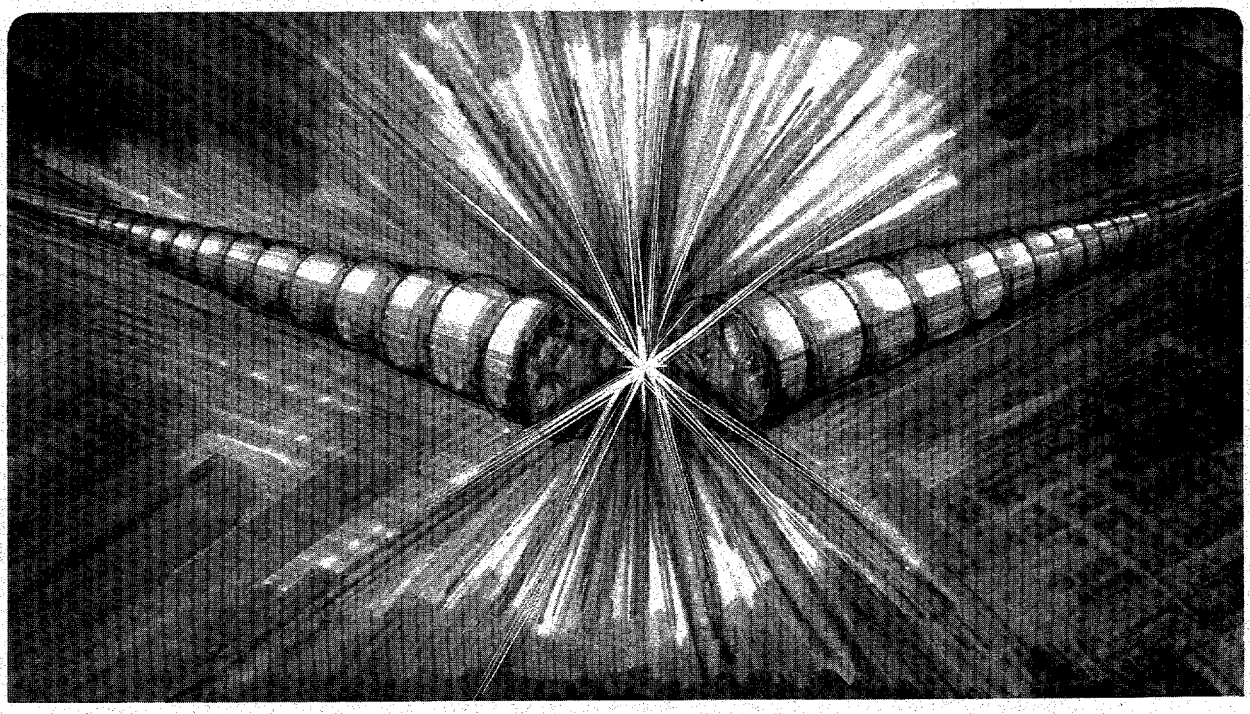

Prepared for the U.S. Department of Energy under Contract Number DE-AC03-76SF00098

LBL-38422
LSBL-314
UC-401

ANGLE-RESOLVED PHOTOEMISSION EXTENDED FINE STRUCTURE STUDY OF CHEMISORBED c(2X2)P/Fe(100): COMPARISON WITH SELF-CONSISTENT-FIELD Xα SCATTERED WAVE CALCULATIONS*

W.R.A. Huff[a,b], Y. Chen[c], X.S. Zhang, L.J. Terminello[d], F.M. Tao[e], Y.K. Pan[e], S.A. Kellar[a,b], E.J. Moler[a,b], Z. Hussain[a], H. Wu, Y. Zheng, X. Zhou[c], A.E. Schach von Wittenau[d], S. Kim, Z.Q. Huang, Z.Z. Yang, and D.A. Shirley[c]

[a]Advanced Light Source, Lawrence Berkeley National Laboratory, University of California, Berkeley, CA 94720

[b]The University of California, Department of Chemistry, Berkeley, CA 94720

[c]The Pennsylvania State University, Department of Chemistry and Physics, University Park, PA 16802

[d]Present address: Lawrence Livermore National Laboratory, Livermore, CA 94550

[e]Boston College, Department of Chemistry, Chestnut Hill, MA 02167

*This work was supported by the Director, Office of Energy Research, Office of Basic Energy Sciences, Chemical Sciences Division, of the U.S. Department of Energy, under Contract No. DE-AC03-76SF00098.

ANGLE-RESOLVED PHOTOEMISSION EXTENDED FINE STRUCTURE STUDY OF CHEMISORBED c(2x2)P/Fe(100): COMPARISON WITH SELF-CONSISTENT-FIELD Xα SCATTERED WAVE CALCULATIONS

W.R.A. Huff,[a,b] Y. Chen,[c] X.S. Zhang, L.J. Terminello,[d] F.M. Tao,[e] Y.K. Pan,[e] S.A. Kellar,[a,b] E.J. Moler,[a,b] Z. Hussain,[a] H. Wu, Y. Zheng, X. Zhou,[c] A.E. Schach von Wittenau,[d] S. Kim, Z.Q. Huang, Z.Z. Yang, and D.A. Shirley[c]

[a]Lawrence Berkeley National Laboratory, Berkeley, CA 94720
[b]The University of California, Dept. of Chemistry, Berkeley, CA 94720
[c]The Pennsylvania State University, Dept. of Chem. and Physics, University Park, PA 16802
[d]Present address: Lawrence Livermore National Laboratory, Livermore, CA 94550
[e]Boston College, Dept. of Chemistry, Chestnut Hill, MA 02167

ABSTRACT

Angle-resolved photoemission extended fine structure (ARPEFS) was used to determine the structure of c(2x2)P/Fe(100) for the first time. P 1*s* core-level photoemission data were collected normal to the (100) surface and 45° off-normal along the [011] direction at room temperature. A close analysis of the auto-regressive linear prediction based Fourier transform and multiple-scattering spherical-wave calculations indicate that the P atoms adsorb in the high-coordination four-fold hollow sites. The P atoms bond 1.02 Å above the first layer of Fe atoms and the Fe-P-Fe bond angle is 140.6°. Additionally, it was determined that there is no expansion of the Fe surface. Self-consistent-field Xα scattered wave calculations were performed for the c(2x2)P/Fe(100) and the c(2x2)S/Fe(100) systems. These independent results are in excellent agreement with this P/Fe structure and the S/Fe structure previously published, confirming the ARPEFS determination that the Fe_1-Fe_2 interlayer spacing is contracted from the bulk value for S/Fe but not for P/Fe.

INTRODUCTION

Angle-resolved photoemission extended fine structure (ARPEFS), scanned energy photoelectron diffraction, is a technique proven to yield accurate, local structural information of atomic and molecular adsorbates on single crystal surfaces to very high precision.[1-5] In addition to determining the adsorbate structure, ARPEFS is able to detect any relaxation of the first few layers of the substrate. By analyzing the auto-regressive linear prediction (ARLP) based Fourier transform (FT),[6,7] the binding site and a reasonably accurate structure can be determined. This allows for a close estimate of the structure without the need for theoretical calculations. Using this estimate as a starting point, multiple-scattering spherical-wave calculations can then be used to determine the structure to high precision (~±0.02 Å).

Self-consistent-field Xα scattered wave (SCF-Xα-SW) calculations were performed for the c(2x2)P/Fe(100) and the c(2x2)S/Fe(100)[4] systems. The SCF-Xα-SW formalism developed by Slater[8] and Johnson[9,10] seems to be a convenient compromise between the need for rigorous calculations and the limitations of computing resources. The SCF equation is solved numerically; the numerical solution is made possible by the Xα approximation for the exchange contribution to the total potential and the muffin-tin approximation for molecular potential and charge densities. The tremendous orbital sizes in these clusters make *ab initio* methods virtually impossible to apply and so the Xα-SW method is the highest level of theory practically available for this work. In fact, the Xα-SW method is particularly appropriate because of the high symmetry of the clusters for the calculations.

EXPERIMENTAL

The experiments were performed in an ultra-high vacuum chamber at pressures ≤60 nPa using beamline 3-3 at the Stanford Synchrotron Radiation Laboratory. The sample was mounted on a high precision (x, y, z, θ, ϕ) manipulator; it was cleaned by repetitive cycles of Ar^+ ion sputtering and subsequent annealing by electron bombardment from behind to ~970 K. The temperature was monitored with a chromel-alumel thermocouple attached near the sample and calibrated with an infrared pyrometer. The LEED pattern of the clean surface showed a clear and sharp (1x1) pattern. The surface contamination level was within the noise level of the measurements both before and after the data acquisition. The c(2x2) phosphorus overlayer was prepared by exposing the surface to PH_3 gas using an effusive beam doser and then annealing the sample to 770 K.

The photoemission spectra were collected using an angle-resolving electrostatic hemispherical electron energy analyzer (mean radius of 50 mm) which is rotatable 360° around the sample's vertical axis and 100° around the sample's horizontal axis. The analyzer pass energy was set to 160 eV and the energy resolution was approximately 1.6 eV FWHM. The angular resolution of the double einzel input lens was ±3°.

DATA ACQUISITION AND ANALYSIS

The photoemission data were collected in two different experimental geometries. In the first data set, the photoemission angle was normal to the Fe(100) surface, i.e. the [001] direction, and the photon polarization vector was 35° from the surface normal. This geometry gives information which is most sensitive to the Fe atoms directly below the P atoms. It could be a first layer Fe atom if P adsorbs in an atop site or a second layer Fe atom if P adsorbs in a four-fold hollow site. If P adsorbs in a bridge site, then the data will be very different. The second set of photoemission data was collected along the [011] direction, i.e. 45° off normal toward the (110) crystallographic plane, and the photon polarization vector was oriented parallel to the emission angle. Schematics of these geometries are shown in figure 1. By taking ARPEFS data off-normal, the structure parallel to the surface is enhanced. Thus, curves from the three possible adsorption sites listed above will appear significantly different. Analyzed together, the two different experimental geometries allow for an accurate determination of interlayer spacings, bond lengths, and bond angles.

ARPEFS raw data are a series of photoemission spectra with changing photoelectron kinetic energy which was varied from 60 eV to 600 eV (4 $Å^{-1}$ to 12.5 $Å^{-1}$, recorded in equal 0.1 $Å^{-1}$ steps). Each photoemission spectrum was a 20 eV window with the P 1s photopeak (B.E. = 2149 eV) located at the center. The peak was fit with a Voigt function to model the natural linewidth as well as the experimental broadening.[11]

The purpose of fitting the spectra is to extract the most accurate area from the peaks to construct the $\chi(k)$ diffraction curve containing the structural information. $\chi(k)$ is defined by[12]

$$\chi(k) = \frac{I(k)}{I_0(k)} - 1 \qquad (1)$$

where $I(k)$ is the peak area plotted as a function of the peak position in k-space. $I_0(k)$ is a smooth, slowly varying function with an oscillation frequency much lower than $I(k)$ and stems from the contribution of the inelastic scattering processes and the varying atomic cross section.[11] The experimental ARPEFS data thus obtained are plotted in figure 1 along with the best-fit results from the multiple scattering modeling calculations which will be discussed later.

Fourier Analysis

The auto-regressive linear prediction based Fourier transform (ARLP-FT) transforms the diffraction curve from momentum space to real space. In ARPEFS, the positions of the strong

peaks in ARLP-FTs from adsorbate/substrate systems can be predicted with fairly good accuracy using the single-scattering cluster model together with the concept of strong backscattering from atoms located within a cone around 180° from the emission direction. The effective solid angle of this backscattering cone is ~30°-40°; it is not unique, but is operationally defined simply by opening the angle until it can account for the observed FT peaks based on the crystal geometry. Signals from scattering atoms very close to the source atom may be observable even if the scatterers lie outside the nominal backscattering cone.

These FT peaks correspond to path-length differences (PLDs) between the component of the photoemitted wave that propagates directly to the detector and the components which are first scattered by the atomic potentials within this backscattering cone.[2] The scattering takes place inside the crystal and the ARPEFS data must be shifted to account for the inner potential. In ARPEFS modeling calculations, the inner potential is treated as an adjustable parameter and is typically 0 - 15 eV. The inner potential for c(2x2)S/Fe(100) was determined to be 14.5 eV.[4] Thus, before taking the FT, the ARPEFS data presented here were shifted by 14 eV to higher kinetic energy.

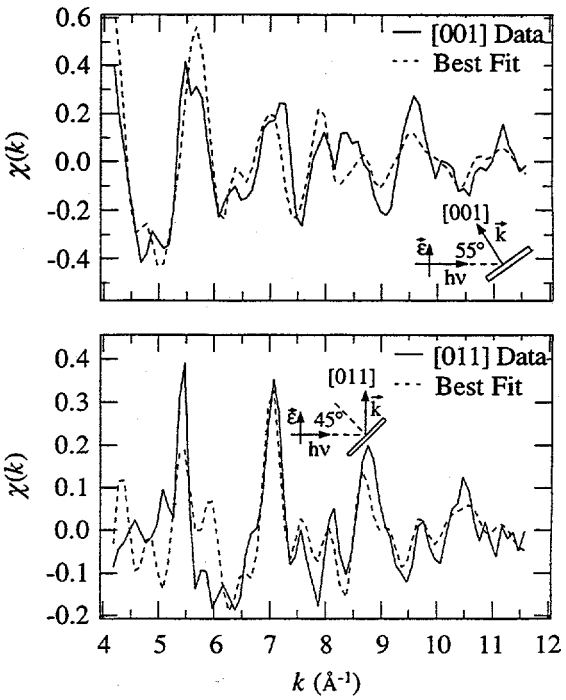

Fig. 1: ARPEFS data from P 1*s* core-level for c(2x2)P/Fe(100) in the [001] and [011] directions. Schematics of each experimental geometry are shown. Dashed lines are the best-fit multiple scattering modeling calculation results.

Without knowing anything about the structure, an analysis of the normal and off-normal ARLP-FTs shown in figure 2 can yield insight to the adsorption site as well as to the bond distance. The sharp c(2x2) LEED pattern suggests that the monolayer coverage is 50% and that the P atoms adsorb on a high symmetry site such as atop, bridge, or four-fold hollow. Using the bulk Fe interlayer spacing, 1.43 Å, the strong peak at 4.77 Å in the [001] FT can be used as a calibration to calculate the distance between the P layer and the first Fe layer for each possible adsorption site. This estimation ignores the small phase shift effects. The PLDs and scattering angles for the strong scattering events can then be calculated using simple geometry and the results for each adsorption site can compared to the [001] and [011] data FTs.

Carefully analyzing the ARLP-FT shows the best agreement if the P atoms adsorb in a four-fold hollow site and the data peak at 4.77 Å is due to backscattering from the *second* layer Fe atoms. For this geometry, the calculated PLDs are in good agreement with the data and the scattering angles are reasonable for the relative strengths of each peak. In fact, from the structure analysis of c(2x2)S/Fe,[4,13,14] it is expected that the P atoms adsorb in the four-fold hollow sites and are ~1 Å above the first layer Fe atoms.

The ARLP-FTs for both the [001] and the [011] data sets are presented in figure 2. Also shown in figure 2 is a schematic of the crystal with

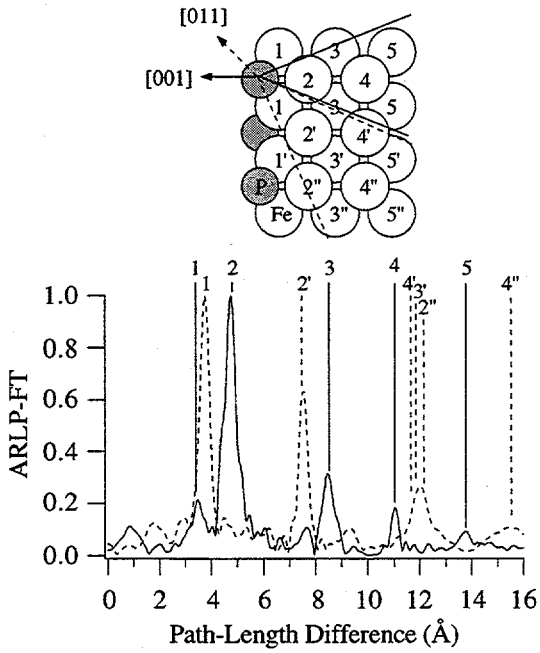

Fig. 2: ARLP-FTs of the ARPEFS [001] data (solid line) and [011] data (dashed line). A model of the lattice with the backscattering cones for each emission direction indicates the scattering atoms corresponding to the FT peaks.

the backscattering cone for each emission direction superimposed; the labeled atoms correspond to labeled peaks in each FT . The solid lines indicate the scattering atoms for [001] photoemission while the dashed lines indicate the scattering atoms for [011] photoemission. Peaks arise in the FT due to scattering from atoms up to five layers below the emitting atoms.

Multiple Scattering Analysis

Modeling calculations were performed to simulate the ARPEFS $\chi(k)$ curve and obtain a structure more precise than yielded by the FT analysis. A new code developed by Chen, Wu, and Shirley was used for the multiple-scattering spherical-wave (MSSW) calculations presented here.[2,12,15-17] The calculations require both structural and nonstructural input parameters. The initial structural parameters were determined from the FT analysis. The nonstructural parameters included were the initial state, the atomic scattering phase shifts, the crystal temperature, the inelastic mean free path, the emission and polarization directions, the electron analyzer acceptance angle, and the inner potential.

To account for vibration effects of the bulk atoms, the mean square relative displacement (MSRD) was calculated and the correlated Debye temperature was set to 400 K.[18,19] The atomic-scattering phase shifts were calculated in situ by using the atomic potentials tabulated by Moruzzi *et al.*[20] The emission and polarization directions and the electron analyzer acceptance angle were set to match the experiment as described earlier. The inelastic mean free path was included using the exponential damping factor $e^{-r/\lambda}$ where λ was calculated using the Tanuma, Powell, and Penn (TPP-2) formula.[21]

The 'multi-curve fitting' feature means that multiple data curves can be fit simultaneously. Figure 1 illustrates the best fit (dashed lines) to both the [001] and the [011] ARPEFS data sets (solid lines) by simultaneous fitting. For these fits, a 76 atom cluster was used and the P-Fe_1 interlayer spacing was determined to be 1.02(2) Å. The inner potential was 15.0 eV. The fitting also determined that there was no relaxation of the first or second Fe layers from the bulk 1.43 Å interlayer spacing. An attempt was made to fit the ARPEFS data using an atop adsorption site and a bridge adsorption site but the fits were very poor for each. The four-fold hollow adsorption site and the P-Fe_1 interlayer spacing for this c(2x2)P/Fe(100) structure correlate well with the structure for chemisorbed c(2x2)S/Fe(100).[4,13,14]

The best fit is determined by an R-factor minimization.[15,22] While fitting, the largest effects stem from changes in the inner potential and the P-Fe_1 interlayer spacing. Figure 3 shows a contour plot of the R-factor as the inner potential and P-Fe_1 interlayer spacing are varied. Analysis of figure 3 indicates that the precision of ARPEFS is ~±0.02 Å, but only if the inner potential is known very well. If, however, the inner potential is allowed to float without constraint, the precision of ARPEFS drops to ~±0.03 Å.

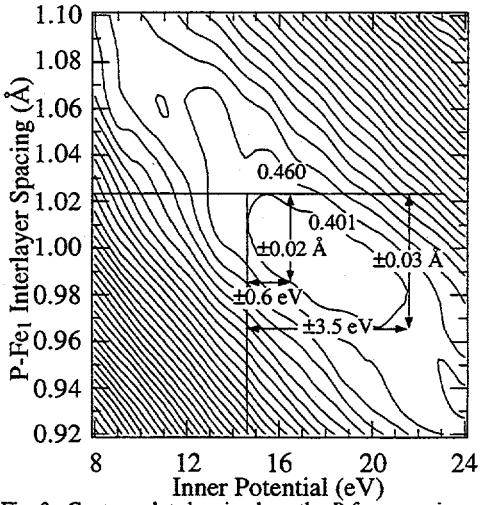

Fig. 3: Contour plot showing how the R-factor varies with the P-Fe_1 interlayer spacing and the inner potential when simultaneously fitting the [001] and [011] ARPEFS data.

SCF-Xα-SW CALCULATIONS

The chemisorption structure of c(2x2)P/Fe(100) and c(2x2)S/Fe(100)[4] from the experimental determination may be further confirmed by theoretical calculations in an appropriate model. In this section, we present SCF-Xα-SW[23-28] calculations on two atomic

clusters, PFe_9 and SFe_9, which represent the two chemisorption systems P/Fe and S/Fe, respectively.

All standard non-empirical parameters for the calculations were used. The radii of atomic spheres were chosen according to Norman[29] and the α exchange parameters were taken from Schwarz's[30] tabulations. In the intersphere and outersphere regions, an average value of α, obtained from a valence-weighted average of the α's for the atoms in the cluster, is employed. Figure 4 shows the structures of the two clusters PFe_9 and SFe_9. The overall symmetry for each cluster is C_{4v}. The four Fe atoms in the top layer are labeled by Fe_1 and the five Fe atoms in the second layer are labeled by Fe_2. The distance of the adsorbed atom P (or S) to the plane formed by the Fe_1 atoms is P-Fe_1 (or S-Fe_1) and the distance between the first and the second layers of Fe atoms is Fe_1-Fe_2. The total energies of the clusters were calculated at several P-Fe_1 (S-Fe_1) distances embracing the experimental equilibrium distance while the Fe_1-Fe_2 interlayer distance was kept at the experimental value. The total energy for a different Fe_1-Fe_2 interlayer distance was also calculated at the experimental P-Fe_1 (S-Fe_1) distance to compare the structural difference in the Fe_1-Fe_2 layer between the P/Fe and the S/Fe systems. The calculation results are presented in the following table for PFe_9 and SFe_9.

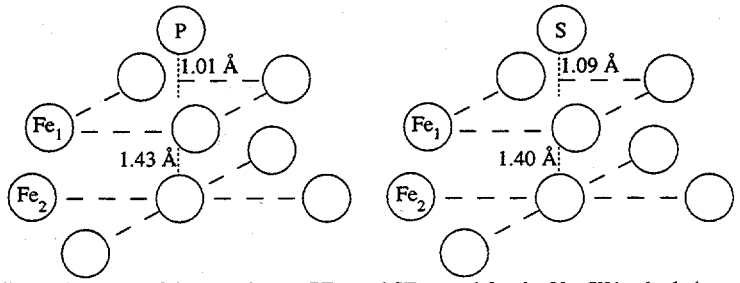

Fig. 4: Structure of the two clusters PFe_9 and SFe_9 used for the Xα-SW calculations.

It is seen in the following table that the P-Fe_1 interlayer distance at the energy minimum is around 1.01 Å with the Fe_1-Fe_2 interlayer distance set at the bulk value of 1.43 Å. This result is consistent with the experimentally obtained structure. Similar good agreement is shown between the calculations and experiment for the S/Fe[4] system where the S-Fe_1 interlayer distance at the energy minimum is around 1.09 Å with the Fe_1-Fe_2 interlayer distance set at the experimentally determined value of 1.40 Å.

These calculation results confirm the ARPEFS determination that the Fe_1-Fe_2 interlayer spacing is contracted from the bulk value for S/Fe but not for P/Fe. If the Fe_1-Fe_2 interlayer spacing is contracted to 1.40 Å for the P/Fe system, the total energy is raised by 1.38 eV. Similarly, if the Fe_1-Fe_2 interlayer spacing is fixed at the 1.43 Å bulk value for the S/Fe system, the total energy is raised by 3.82 eV. The bottom row lists the calculated energy with Fe_1-Fe_2 fixed at 1.40 Å for P/Fe and 1.43 Å for S/Fe.

c(2x2)P/Fe(100)			c(2x2)S/Fe(100)		
P-Fe_1 (Å)	Energy (eV)	ΔE (eV)	S-Fe_1 (Å)	Energy (eV)	ΔE (eV)
1.06	-318411.46	1.89	1.14	-319983.03	2.39
1.04	-318412.48	0.87	1.12	-319984.57	0.85
1.01	-318413.35	0	1.09	-319985.42	0
0.99	-318410.35	3.00	1.07	-319984.40	1.02
1.01	-318411.97	1.38	1.09	-319981.60	3.82

CONCLUSION

Angle-resolved photoemission extended fine structure was used to determine the structure of c(2x2)P/Fe(100) for the first time. Photoemission data were collected normal to the (100) surface and 45° off-normal along the [011] direction at room temperature. A close analysis of the ARLP based FT indicates that the P atoms adsorb in the high-coordination four-fold hollow sites. The multiple-scattering spherical-wave calculations which simulate the photoelectron diffraction confirmed the four-fold hollow adsorption site. By simultaneously fitting both ARPEFS data sets, the P atoms were determined to bond 1.02(2) Å above the first layer of Fe atoms. The Fe-P-Fe bond angle is thus 140.6°. Assuming the radius of the Fe atoms is 1.24 Å, the effective P radius is 1.03 Å. The inner potential was 15.0 eV. It was also determined that

there was no relaxation of the first or second Fe layers from the bulk 1.43 Å interlayer spacing. To test this fitting method, each data set was fit individually and these results were in good structural agreement.

Additionally, self-consistent-field Xα scattered wave calculations were performed for the c(2x2)P/Fe(100) and the c(2x2)S/Fe(100)[4] systems. These independent results are in excellent agreement with this P/Fe structure and the S/Fe structure previously published, confirming the ARPEFS determination that the Fe_1-Fe_2 interlayer spacing is contracted from the bulk value for S/Fe but not for P/Fe.

ACKNOWLEDGMENTS

This work was supported by the Director, Office of Energy Research, Office of Basic Energy Sciences, Chemical Sciences Division of the U.S. Department of Energy under Contract No. DE-AC03-76SF00098. It was performed at the Stanford Synchrotron Radiation Laboratory which is supported by the Department of Energy's Office of Basic Energy Sciences.

REFERENCES

[1]D.P. Woodruff, D. Norman, B.W. Holland, N.V. Smith, *et al.*, Phys. Rev. Lett. **41**, 1130(1978).
[2]J.J. Barton, C.C. Bahr, S.W. Robey, Z. Hussain, E. Umbach and D.A. Shirley, Phys. Rev. B **34**, 3807(1986).
[3]S.W. Robey, J.J. Barton, C.C. Bahr, G. Liu and D.A. Shirley, Phys. Rev. B **35**, 1108(1987).
[4]X.S. Zhang, L.J. Terminello, S. Kim, Z.Q. Huang, A.E. Schach von Wittenau and D.A. Shirley, J. Chem. Phys. **89**, 6538(1988).
[5]Z.Q. Huang, Z. Hussain, W.T. Huff, E.J. Moler and D.A. Shirley, Phys. Rev. B **48**, 1696(1993).
[6]J.J. Barton, C.C. Bahr, Z. Hussain, S.W. Robey, J.G. Tobin, L.E. Klebanoff and D.A. Shirley, Phys. Rev. Lett. **51**, 272(1983).
[7]J.J. Barton, Z. Hussain and D.A. Shirley, Phys. Rev. B **35**, 933(1987).
[8]J.C. Slater, Phys. Rev. **81**, 385(1951).
[9]K.H. Johnson, J. Chem. Phys. **45**, 3085(1966).
[10]K.H. Johnson, Adv. Quantum Chem. **7**, 143(1972).
[11]J.J. Barton, *Ph.D. Thesis*, The University of California, Berkeley, LBL-19215(1985).
[12]J.J. Barton, S.W. Robey and D.A. Shirley, Phys. Rev. B **34**, 778(1986).
[13]K.O. Legg, F. Jona, D.W. Jepsen and P.M. Marcus, Surf. Sci. **66**, 25(1977).
[14]R.A. DiDio, E.W. Plummer and W.R. Graham, J. Vac. Sci. Technol. **A2**, 983(1984).
[15]Y. Chen, H. Wu and D.A. Shirley, *MSSW Code - Unpublished*, (1995).
[16]J.J. Rehr and R.C. Albers, Phys. Rev. B **41**, 8139(1990).
[17]M. Biagini, Phys. Rev. B **48**, 2974(1993).
[18]M. Sagurton, E.L. Bullock and C.S. Fadley, Surf. Sci. **182**, 287(1987).
[19]R.E. Allen, G.P. Alldredge and F.W. de Wette, J. Chem. Phys. **54**, 2605(1971).
[20]V.L. Moruzzi, J.F. Janak and A.R. Williams, *Calculated Electronic Properties of Metals*, (Pergamon Press, Inc., New York, 1978).
[21]S. Tanuma, C.J. Powell and D.R. Penn, Surf. Interface Anal. **20**, 77(1993).
[22]W.H. Press, S.A. Teukolsky, W.T. Vetterling and B.P. Flannery, *Numerical Recipes in Fortran: The Art of Scientific Computing*, 2 ed., (University Press, Cambridge, 1992).
[23]M. Cook and M. Karplus, J. Chem. Phys. **72**, 7(1980).
[24]D.A. Case, M. Cook and M. Karplus, J. Chem. Phys. **73**, 3294(1980).
[25]M.E. Eberhart, K.H. Johnson and D. Adler, Phys. Rev. B **26**, 3138(1982).
[26]J.S.-Y. Chao and K.D. Jordan, J. Phys. Chem. **91**, 5578(1987).
[27]M. Cook and C.T. White, Phys. Rev. B **38**, 9674(1988).
[28]H. Adachi and M. Takano, J. Solid State Chem. **93**, 556(1991).
[29]Jr. J.G. Norman, Mol. Phys. **31**, 1191(1976).
[30]K. Schwarz, Phys. Rev. B **5**, 2466(1972).